Molecular Neurobiology (2019) 56:1248–1261
https://doi.org/10.1007/s12035-018-1167-9

Neuronal and Glial Differentiation of Human Neural Stem Cells Is Regulated by Amyloid Precursor Protein (APP) Levels

Raquel Coronel[1] · María Lachgar[1] · Adela Bernabeu-Zornoza[1] · Charlotte Palmer[1] · Marta Domínguez-Alvaro[1] · Ana Revilla[1] · Inmaculada Ocaña[1] · Andrés Fernández[2] · Alberto Martínez-Serrano[3] · Eva Cano[2] · Isabel Liste[1]

Received: 12 January 2018 / Accepted: 30 May 2018 / Published online: 7 June 2018

Abstract

Amyloid precursor protein (APP) is implicated in neural development as well as in the pathology of Alzheimer's disease (AD); however, its biological function still remains unclear. It has been reported that APP stimulates the proliferation and neuronal differentiation of neural stem cells (NSCs), while other studies suggest an important effect enhancing gliogenesis in NSCs. As expected, APP protein/mRNA is detected in hNS1 cells, a model cell line of human NSCs, both under proliferation and throughout the differentiation period. To investigate the potential function that APP plays in cell fate specification and differentiation of hNS1 cells, we transiently increased human APP levels in these cells and analyzed its cell intrinsic effects. Our data indicate that increased levels of APP induce early cell cycle exit and instructively direct hNS1 cell fate towards a glial phenotype, while decreasing neuronal differentiation. Since elevated APP levels also enhanced APP intracellular domain (AICD)-immunoreactivity, these effects could be, in part, mediated by the APP/AICD system. The AICD domain can play a potential role in signal transduction by its molecular interaction with different target genes such as *GSK3B*, whose expression was also increased in APP-overexpressing cells that, in turn, may contribute to promoting gliogenesis and inhibiting neurogenesis in NSCs. These data suggest an important action of APP in modulating hNSCs differentiation (probably in an AICD-GSK-3β-dependent manner) and may thus be important for the future development of stem cell therapy strategies for the diseased mammalian brain.

Keywords Human neural stem cells · Amyloid precursor protein · Cell fate · Differentiation · Neurogenesis · Gliogenesis

Introduction

One of the major components of amyloid plaques present in brains of neurological conditions, such as Alzheimer's disease (AD), Down syndrome (DS), and brain injury, is the Aβ peptide (Aβ), a derivative of the amyloid precursor protein (APP) [1, 2]. The involvement of APP in the pathology of AD has been well documented, but there is still no clear consensus about its physiological function [3]. APP is a type I integral transmembrane glycoprotein, encoded by a single gene located on chromosome 21. This protein is ubiquitously expressed in a wide variety of tissues, being especially abundant in the brain [4]. Several alternative splice forms of APP have been identified so far, and APP695 is the form predominantly expressed in the developing central nervous system (CNS) [1, 5]. The expression of APP is detected at early stages of nervous system development [6, 7], suggesting an important role of this protein in neural growth and maturation.

Recent findings have also brought to light possible functions of APP in the adult brain, such as the regulation of neural progenitor cell proliferation [8] and axonal outgrowth after injury [9], indicating a neurogenic and neuro-regenerative role of APP in the brain. There is evidence that APP can act as a trophic factor during neurite outgrowth and synaptogenesis

Electronic supplementary material The online version of this article (https://doi.org/10.1007/s12035-018-1167-9) contains supplementary material, which is available to authorized users.

✉ Isabel Liste
iliste@isciii.es

[1] Unidad de Regeneración Neural, Unidad Funcional de Investigación de Enfermedades Crónicas, Instituto de Salud Carlos III (ISCIII), Majadahonda, 28220 Madrid, Spain

[2] Unidad de Neuroinflamación, Unidad Funcional de Investigación de Enfermedades Crónicas, Instituto de Salud Carlos III (ISCIII), Majadahonda, Madrid, Spain

[3] Centro de Biología Molecular "Severo Ochoa" (CBMSO), Universidad Autónoma de Madrid-Consejo Superior de Investigaciones Científicas (UAM-CSIC), Campus UAM Cantoblanco, Madrid, Spain

[10–12], neuronal migration [13], and neurogenesis both in vitro [2, 14–16] and in vivo in adult transgenic mice overexpressing human APP [17, 18]. However, the cellular and molecular mechanisms by which APP regulates these processes remain poorly understood.

APP protein can be processed by two different pathways, the non-amyloidogenic and the amyloidogenic pathway. The non-amyloidogenic pathway is driven by α-secretase cleavage, which releases the soluble APPα protein (sAPPα), avoiding Aβ generation after γ-secretase activity. In the amyloidogenic pathway, the Aβ peptide is generated from sequential cleavage of APP by β-secretase, generating the soluble APPβ protein (sAPPβ). The remaining C-terminal region is processed by a γ-secretase that results in the release of the Aβ peptide. It is thought that the APP intracellular domain (AICD) obtained by both pathways can be translocated into the nucleus to regulate the expression of different target genes such as *BACE1*, *ADAM10*, *KAI1*, and *GSK3B* [1, 2, 19].

The soluble forms of secreted APP (mainly sAPPα) have shown to be neuroprotective and important for neurogenesis [8, 20, 21], and it has been suggested that AICD has a regulatory role in neuronal cell proliferation and differentiation [22, 23]. Specifically, AICD has been found to negatively modulate neurogenesis in neural stem/precursor cells, though the mechanism is still poorly understood [2, 24, 25].

Human neural stem cells (hNSCs) are precursors of neurons and glia, and generate all the differentiated neural cells of the CNS. These cells can be sourced from the fetal, neonatal, and adult brain, or from directed differentiation of pluripotent stem cells [26, 27]. hNSCs have become a useful tool to help the progress of clinical applications for stem cell-based therapies for several neurodegenerative disorders, and have also provided a better understanding of human brain development and the molecular pathology associated with neurodegeneration [28].

In the present study, we aimed to identify the intrinsic cellular effects of APP in the differentiation process and cell fate specification of hNSCs. To achieve this, we used hNS1 cells, a clonal model cell line of hNSCs obtained from the human fetal forebrain [29–31]. We observed that APP overexpression promoted gliogenesis, while inhibiting neuronal differentiation in hNS1 cells. These findings indicate that increasing APP levels can regulate the biology and differentiation potential of hNSCs by affecting their cell fate specification.

Materials and Methods

Ethics Statement

The original human tissues were donated for research after written informed consent of women seeking abortion. Tissue procurement was made in accordance with the Declaration of Helsinki and in accordance with the ethical standards of the Network of European CNS Transplantation and Restoration (NECTAR). Approval to use theses tissues for research was granted by the University of Lund Hospital Ethics Committee, and its use was in compliance with Spanish Law 35/1988 on Assisted Reproduction. Ethics statements on human fetal origin of cells used in this study can be found in the original reports describing the hNS1 cell line [29, 31].

Cell Culture

We used hNS1 cells, a model of hNSCs that has been previously characterized [29–31]. This cell line is a v-myc immortalized, non-transformed, human fetal forebrain-derived, multipotent, and clonal cell line of human neural stem cells. hNS1 cell culture conditions are based on a chemically defined human stem cell (HSC) medium supplemented with 20 ng/ml epidermal growth factor (EGF; PetroPech) and 20 ng/ml basic fibroblast growth factor (FGF2; PetroPech) [31]. Cells were proliferated in an incubator set to 37 °C and 5% CO_2 (Forma). Cultures were differentiated on poly-L-lysine- (10–30 μg/ml; Sigma) coated plastic or glass coverslips, by withdrawal of growth factors (EGF and FGF2) and addition of 0.5% heat-inactivated fetal bovine serum (FBS) for the indicated times.

Some cultures were treated with the GSK-3 inhibitor CHIR99021 (3 and 5 μM; TOCRIS) dissolved in DMSO (vehicle) from the beginning of differentiation to day 4. Schematic view is represented in Fig. 6a.

APP Overexpression in hNS1 Cells

We studied the effects of APP on a short time scale (days after nucleofection). To this end, we nucleofected (Amaxa nucleofector II Kit, program A031, following manufacturer recommendations) control hNS1 cells with 4 μg of an empty plasmid (pcDNA.3-Empty; Invitrogen) or 4 μg of a plasmid containing the gene for APP695 (pcDNA.3-APP695; kindly provided by Dr. Daniel Lu, UCLA). These plasmids were co-nucleofected with 4 μg of a plasmid containing green fluorescent protein (GFP) (pCAG-GFP; Addgene) to track transfected cells. Cells were plated in proliferation medium (day −2) and differentiation was started at day 0 by adding regular differentiation medium. Cells were differentiated until day 4 or 7 (as indicated in each experiment).

It is important to note that in order to confirm plasmid co-transfection, a control study was performed where hNS1 cells were co-nucleofected with 2 μg of the pCAG-GFP plasmid and 2μg of a plasmid containing red fluorescent protein (RFP) (pCAG-RFP; Addgene) (Supplementary Fig. 2).

Immunocytochemistry and Immunoblotting

At the specified time points, the cultures were rinsed with PBS and fixed for 10 min in freshly prepared 4% PFA. Cultures were blocked for 1 h in 5% normal horse serum with 0.25% Triton X-100 in PBS and incubated overnight at 4 °C with mouse monoclonal antibodies against β-III-tubulin (class III β-tubulin; 1:500; Biolegend #801202) and GFAP (glial fibrillary acid protein; 1:1000; BD Pharmigen #556327), or rabbit antibodies against Sox2 (1:500; Millipore #AB5603), Ki67 (1:500; Thermo Scientific #MA5-14520), Nestin (1:500; Sigma #N5413), β-III-tubulin (1:500; Sigma #T2200), or GFAP (1:1000; Dako #Z0334). For APP detection, several antibodies (see Fig. 2a) raised against different APP protein epitopes were used:

- Mouse monoclonal APP (clone 22C11) (1:500; Millipore #MAB348). It is reactive to amino acid residues 66–81 of APP (N-terminus), detecting APP (full length and soluble forms).
- Mouse monoclonal APP (clone 4G8) (1:250; Biolegend #800701). It is reactive to amino acid residues 17–24 of Aβ peptide and identifies Aβ peptide and full length APP.
- Mouse monoclonal anti-human APP (clone 6E10) (1:1000; Biolegend #803004). It is reactive to amino acid residue 1–16 of Aβ peptide, detecting full length APP and Aβ peptide.
- Rabbit anti-APP (C-terminal region) (1:100; Aviva Biosystems #ARP32591_P050). It detects the C-terminal domain of human APP.

The cultures were then incubated with Alexa 488-conjugated antibodies (donkey anti-rabbit or donkey anti-mouse, 1:500; Invitrogen #A21206; #A21202) or with Alexa 555-conjugated antibodies (donkey anti-rabbit or donkey anti-mouse, 1:500; Invitrogen #A31572; #A31570). Cell nuclei were counterstained with Hoechst 33258 (Molecular Probes) at 0.2 μg/ml in PBS.

Analysis and photographs of fluorescent-immunostained cultures were carried out in an inverted Leica (Nussloch, Germany) DM IL LED (equipped with a digital camera Leica DFC345FX) microscope. In all experiments, digitalized images were captured using Leica LAS V4.0 software. Image analysis was performed using Photoshop CS6 after randomly capturing at least 10 separate fields per well, with a minimum of three wells per experimental group. In overexpression assays, at least 100 GFP^+ cells were counted per well.

For western blot (WB) analysis, 30–50 μg protein from cellular extracts of dividing or differentiated cultures were assayed. Samples were boiled for 5 min, loaded on a 10% sodium dodecyl sulfate (SDS)-polyacrylamide gel, electrophoresed, and transferred to nitrocellulose membranes (GE Healthcare). Membranes were blocked in 5% non-fat dairy milk with 0.05% Tween20 in TBS for 1 h at room temperature. Blots were incubated overnight at 4 °C with primary antibodies against mouse anti-β-actin (1:1000; Sigma #A5441), mouse anti-APP (clone 22C11; 1:1000; Millipore #MAB348), mouse anti-APP (clone 6E10; 1:1000; Biolegend #803004), mouse anti-APP (C-terminal region; 1:1000; Biolegend #802803), and mouse anti-GSK-3β (1:100; Santa Cruz #SC-377213). The blots were developed using peroxidase-conjugated horse anti-mouse (HAMPO; 1:3000; Vector Laboratories #ZC1212) and developed using the ECL system (Millipore).

For quantification of blot images, densitometry analyses were realized using the software Quantity One. Band intensity was measured as a ratio of the protein of interest to β-actin from three independent experiments.

RNA Isolation and Reverse Transcription PCR

Total RNA was isolated with the RNeasy Mini extraction kit (Qiagen, Valencia, CA, USA) according to manufacturer's instruction and treated with DNAses to avoid amplification of undesired genomic and plasmid DNA. One microgram of total RNA was reverse-transcribed at 50 °C for 60 min, in a 20 μl reaction mixture using SuperScriptIII-RT (Life Technologies, Carlsbad, CA, USA). Fifty nanograms of cDNA was amplified in a 20 μl PCR reaction mixture using Biotaq (BioLine, London, UK) following the subsequent thermal profile: 94 °C 3 min; 40 cycles (94 °C 30s , 50 °C 30 s, 72 °C 1 min); 72 °C 10 min. PCRs were performed using primers for human target genes *ADAM10* (forward: 5′-AGCAACATCTGGGGACAAAC-3′; reverse: 5′-CCCAGGTTTCAGTTTGCATT-3′), *BACE1* (forward: 5′-GGGCAGGGCTACTACGTG-3′; reverse: 5′-CAGCACCCACTGCAAAGTT-3′), *GSK3B* (forward: 5′-ATCCTTGGACTAAGGTCTTCCG-3′; reverse: 5′-GAATAAGGATGGTAGCCAGAGG-3′), and *GAPDH* as a reference gene (forward: 5′-GTCAAGGCTGAGAACGGGAA-3′; reverse: 5′-AAATGAGCCCCAGCCTTCTC-3′). Products were resolved on 2% agarose gels under UV light with GelRed staining (Biotium, Hayward, CA).

To analyze reverse transcription PCR (RT-PCR) data, areas of the bands of the PCR products from three independent experiments (for each gene of interest) were measured using ImageJ software and represented by relative area versus *GAPDH*. Gene expression levels were normalized against *GAPDH* for differences in sample concentration and loading.

Quantitative Real-Time PCR

Relative amounts of cDNA were quantified by quantitative real-time PCR (q-RT-PCR) using the FAST SYBR-green system (Applied Biosystems) according to the manufacturer's protocol. Ten nanograms of total cDNA and 10 μM of primers

were used in a 15 μl reaction mixture. q-RT-PCRs were performed using primers for the follow human target genes: *SOX2* (forward: 5′-GGGGGAATGGACCTTGTATAG-3′; reverse: 5′-GCAAAGCTCCYACCGTACCA-3′), *GFAP* (forward: 5′-GTTCTTGAGGAAGATCCACGA-3′; reverse: 5′-CTTGGCCACGTCAAGCTC-3′), *S100B* (forward: 5′-GGAAGGGGTGAGACAAGGA-3′; reverse: 5′-GGTG GAAAACGTCGATGAG-3′), *TUBB3* (forward: 5′-GCAA CTACGTGGGCGACT-3′; reverse: 5′- ATGGCTCG AGGCACGTACT-3′), *APP* (forward: 5'-GGTTTGGC ACTGCTCCTG-3′; reverse: 5′-CAGTCTGCCACAGA ACATGG-3′), *APP695* (forward: 5′-GACGATGAGGATGG TGATGA-3′; reverse: 5′-CTGGCTGCTGTTGTAGGAACT-3′), *ADAM10* (forward: 5′-ATATTACGGAACACGAGAAG CTG-3′; reverse: 5′-TCAATCGCTTTAACATGACTGG-3′), *BACE1* (forward: 5′-CTTCATCAACGGCTCCAACT-3′; reverse: 5′-AACGTGGGTCTGCTTTACCA-3′), *GSK3A* (forward: 5′-GTCTCCTACATCTGTTCTCGCTACT-3′; reverse: 5′-CAGCCAGCTGACCAAACAT-3′), *GSK3B* (forward: 5′-GAAAGTATTGCAGGACAAGAGATTT-3′; reverse: 5′-CGGACTATGTTACAGTGATCTAGCTT-3′), and housekeeping gene *TBP* (forward: 5′-GAGCTGTGATGTGA AGTTTCC-3′; reverse: 5′-TCTGGGTTTGATCATTCTGT AG-3′). The Applied Biosystems 7500 Real-Time PCR System was used to determine the amount of target mRNA in each sample, estimated by the $2^{-\Delta\Delta Ct}$ relative quantification method. Gene expression levels were normalized against *TBP* levels in each sample.

Statistical Analysis

Statistical tests were run using Graphpad Prism 6.0. Results are shown as the average ± S.E.M. of data from 3 to 4 experiments ($n = 3$ or $n = 4$). Mean values were compared using the Studen's t test for independent samples or one-way ANOVA for multiple comparison. p values < 0.05 were considered to be statistically significant ($*p < 0.05$, $**p < 0.01$, $***p < 0.001$, $****p < 0.0001$).

Results

Endogenous APP Expression During Differentiation of hNS1 Cells

hNS1 cells were differentiated and analyzed at different time points of the differentiation period (Fig. 1a) for the expression and production of the main neural markers: Nestin (neural precursors), Sox2 (neural precursors), β-III-Tubulin (BIIITub, neurons), and GFAP (glial cells). As expected, most of the dividing hNS1 cells were positive for Nestin (96.9 ± 8.0%) and Sox2 (96.3 ± 0.8%), while only a small percentage of cells were GFAP (2.3 ± 1.5%) and BIIITub (2.5 ± 0.4%) positive. We observed that during the time course of differentiation, the percentage of Nestin$^+$ and Sox2$^+$ cells decreased, whereas the number of GFAP$^+$ and BIIITub$^+$ cells increased. At day 14 of differentiation, 45.0 ± 3.1 and 27 ± 6% of total cells were GFAP$^+$ and BIIITub$^+$, respectively, whereas 24.0 ± 4.2% of cells remained Nestin$^+$ and 51.8 ± 2.4% of cells Sox2$^+$ (Fig. 1b, c). Similar markers were investigated in q-RT-PCR, with comparable results (Fig. 1d) and consistent with our previous data [29–31], further confirming the multipotency and differentiation potential of hNS1 cells.

Fig. 1 Differentiation time course of hNS1 cell line. **a** Schematic representation of the protocol used for proliferation (division) and differentiation. **b** Representative images in phase contrast and immunoreactivity for Sox2, Nestin, GFAP, and B-III-Tubulin in dividing and differentiating hNS1 cells (days 3, 7, and 14). Scale bar = 50 μm. **c** Percentage of positive cells for Sox2 (i), Nestin (ii), GFAP (iii), and B-III-Tubulin (iv) with respect to total cells along the differentiation time course of hNS1 cells. Data represent mean ± S.E.M. ($n = 4$ for each experiment; results were confirmed in two independent experiments). Statistical analysis was performed using one-way ANOVA (multiple comparisons of each group vs division group); $*p < 0.05$; $**p < 0.01$; $****p < 0.0001$. **d** Relative expression levels of *SOX2* (i), *GFAP* (ii), *S100B* (astroglial marker) (iii), and *TUBB3* (iv) by q-RT-PCR along the differentiation time course of hNS1 cells. Data represent mean ± S.E.M. ($n = 3$ for each experiment; results were confirmed in two independent experiments). Statistical analysis was performed using one-way ANOVA (multiple comparisons of each group vs division group); $*p < 0.05$; $**p < 0.01$; $***p < 0.001$; $****p < 0.0001$

To examine whether APP is endogenously expressed in hNS1 cells, and if this production was altered during proliferation or differentiation, parallel cultures of proliferating and differentiating cells were fixed and stained using two different antibodies against APP (clones 22C11 and 4G8, see Fig. 2a). In both conditions, APP-immunoreactivity was observed. 98.9 ± 1.0% of dividing cells were APP$^+$, while 82.5 ± 2.1% of cells were APP$^+$ at the end of the differentiation period (Fig. 2b, c). APP protein levels (both the mature (glycosylated) and immature forms) were also observed in cellular extracts of hNS1 cells by WB analysis using two different antibodies against APP (22C11 and 6E10) (Fig. 2d). Interestingly, APP levels seem to increase with differentiation time, as shown both at the protein level (Fig. 2d, e) and as relative mRNA expression (Fig. 2f).

In summary, APP is clearly present in hNS1 cells, both in proliferation and throughout the differentiation process, suggesting a possible function in these cellular processes.

Effects of APP on Cell Fate Specification of hNS1 Cells

To investigate the intrinsic effects of APP in hNS1 cells, we carried out gain-of-function studies by transient APP overexpression. Studies were done on a short time scale, to avoid the likely compensatory mechanisms that could result from stable APP overexpression. After nucleofection with plasmids coding for APP and GFP (APP + GFP; APP group) or with the empty plasmid and GFP plasmid (Empty + GFP; control group),

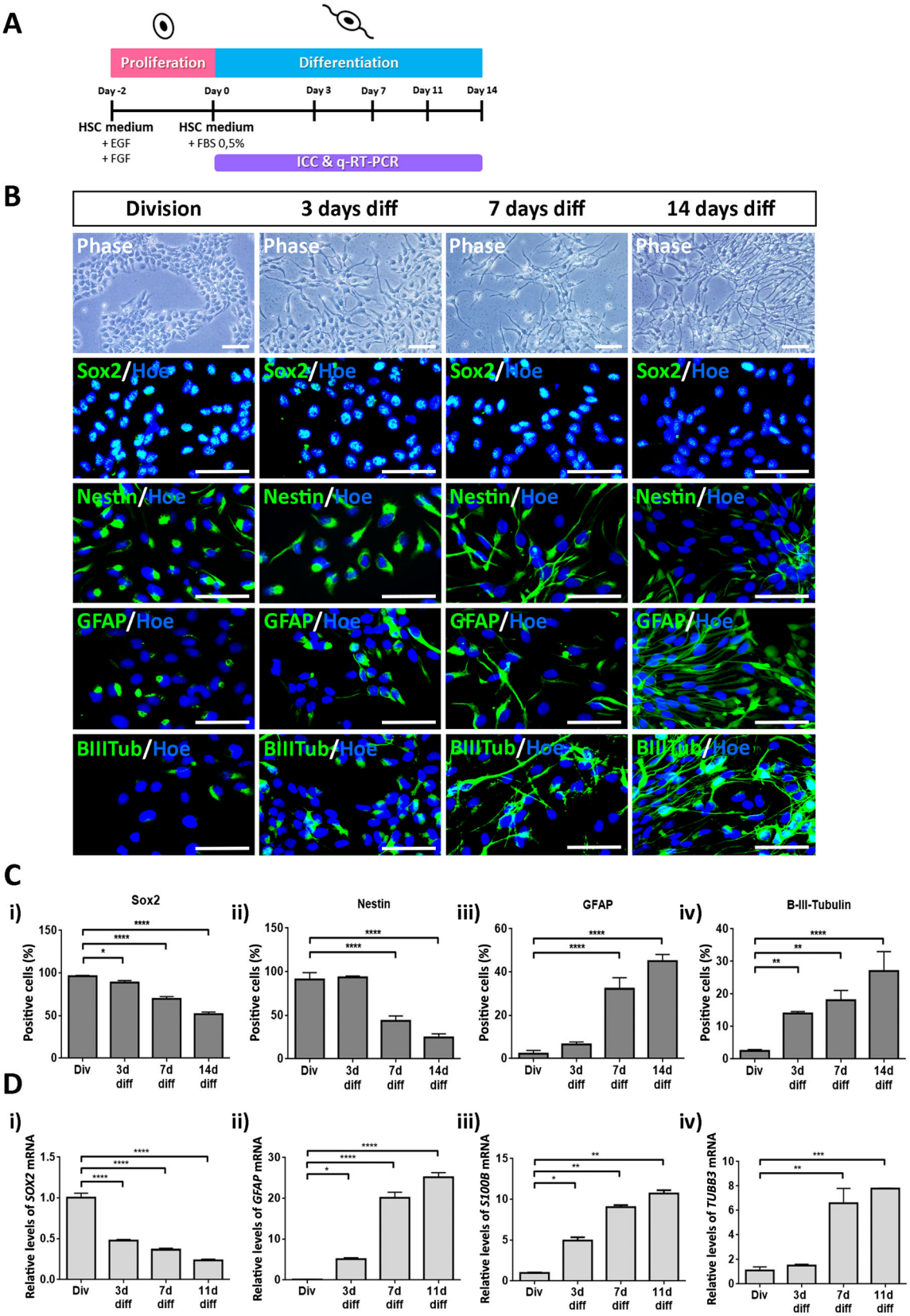

hNS1 cells were differentiated until days 4 and 7 (Fig. 3a). Nucleofection efficiency of both plasmid preparations was equivalent, as determined on day 2 post-nucleofection (between 25 and 28% of GFP$^+$ cells) (Supplementary Fig. 1). Since our

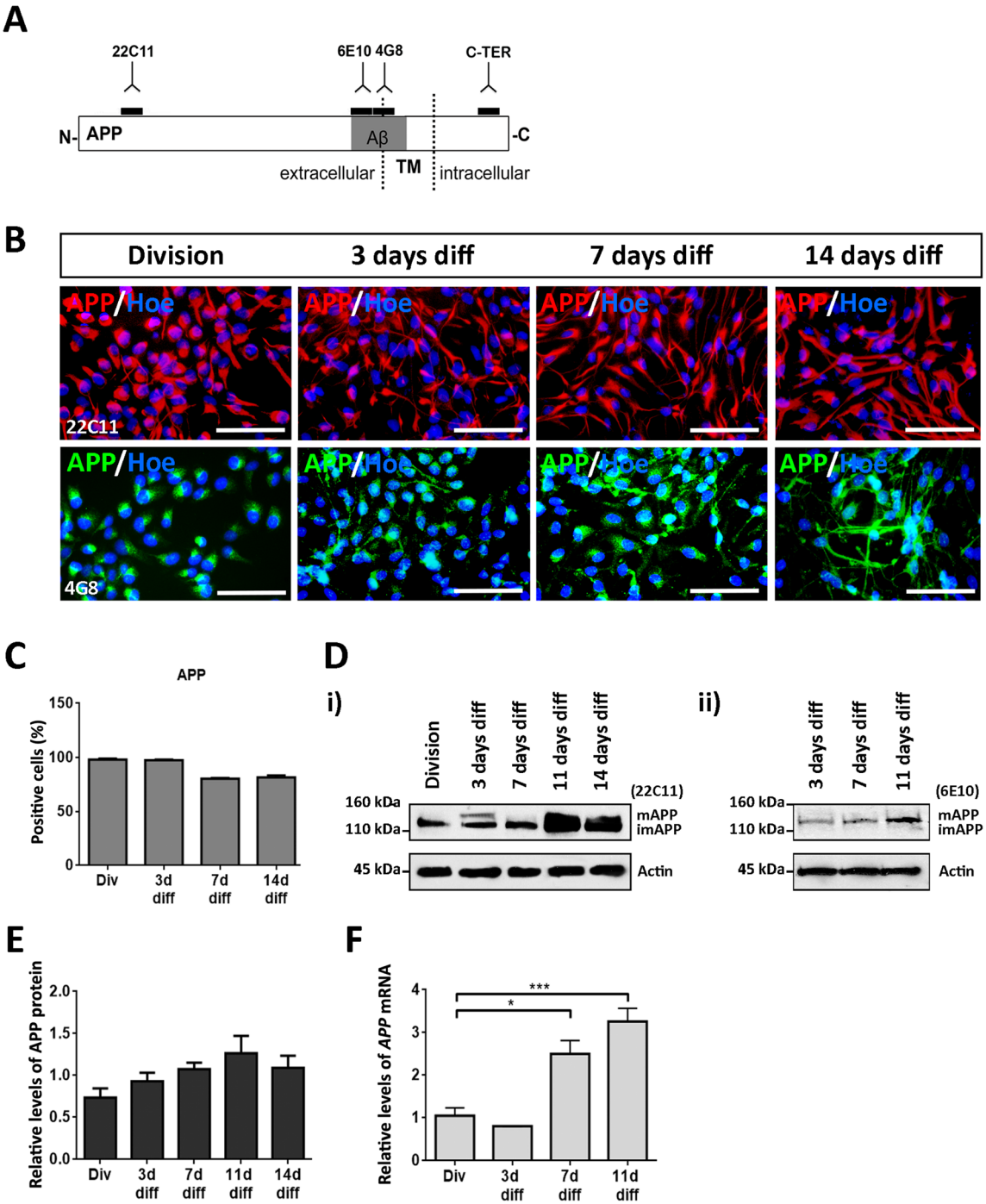

Fig. 2 Expression of APP protein in hNS1 cells during proliferation and differentiation. **a** Schematic representation of the antibodies (22C11; 6E10; 4G8; C-TER) against different APP protein epitopes used in this study: TM (transmembrane region of APP), N (N-terminal region), C (C-terminal region), Aβ (domain of Aβ peptide of APP). **b** Immunoreactivity for endogenous APP (using 22C11 and 4G8 antibodies) in dividing and differentiating hNS1 cells (days 3, 7, and 14). Scale bar = 50 μm. **c** Percentage of positive cells for APP with respect to total cells along the differentiation time course of hNS1 cells. Data represent mean ± S.E.M. ($n = 3$ for each experiment; results were confirmed in two independent experiments). **d** Western blot analysis of endogenous APP (using 22C11 (i) and 6E10 (ii) antibodies) in cellular extracts of diving and differentiating hNS1 cells. Actin was used as a loading control: mAPP (mature APP), imAPP (immature APP). **e** Relative protein levels of APP (clone 22C11) by densitometry analysis along the differentiation time course of hNS1 cells. **f** Relative expression levels of endogenous *APP* by q-RT-PCR along the differentiation time course of hNS1 cells. Data represent mean ± S.E.M. ($n = 3$ for each experiment; results were confirmed in two independent experiments). Statistical analysis was performed using one-way ANOVA (multiple comparisons of each group vs division group); $^{*}p < 0.05$; $^{***}p < 0.001$

preliminary data analyzing the co-transfection efficiency of GFP and RFP expressing vectors showed co-localization of both proteins (Supplementary Fig. 2), we assumed co-transfection of both plasmids in the subsequent analyses.

Q-RT-PCR analysis showed that *APP* mRNA expression is increased in APP-plasmid transfected cells compared to control cells (Fig. 3b). These results were confirmed at the protein level by immunofluorescence against APP in APP nucleofected cells (Fig. 3c) and by WB analysis (Fig. 3d, e), both in dividing and differentiating cultures using two different antibodies (22C11 and 6E10).

To evaluate the possible effect of APP on cycling cells, we stained samples at day 4 of differentiation for Ki67 (cell cycle marker). We observed a notable decrease in $Ki67^+/GFP^+$ cells in the APP group (32.0 ± 1.8%) as compared to the control group (72.0 ± 1.5%) ($p < 0.001$; $n = 4$). A phenotypic analysis of GFP^+ cells counter-staining for GFAP and BIIITub showed that 27 ± 3% of cells in the APP group were $GFAP^+/GFP^+$ as compared to 67.0 ± 1.5% in the control group ($p < 0.001$; $n = 4$) (Fig. 4b, c). On the contrary, the analysis of neuronal generation showed a significant reduction of $BIIITub^+/GFP^+$ cells in the APP group (4.7 ± 0.9%) as compared to the control group (20.3 ± 2.1%) ($p < 0.01$; $n = 4$) (Fig. 4b, c). No statistically significant difference was observed for $Nestin^+/GFP^+$ between the two groups. These results were further confirmed at the level of mRNA expression by q-RT-PCR analysis for *GFAP* and *TUBB3* (Fig 4d).

Together, our results indicate that increased levels of APP in hNS1 cells can promote cell cycle exit, as well as favor the differentiation towards a glial phenotype, while decreasing neuronal differentiation.

To assess whether these effects were maintained or compensated for during the course of differentiation, we analyzed the same groups of cells at differentiation day 7. Our results were consistent with those obtained at differentiation day 4 for GFAP and BIIITub. 96.3 ± 1.8% of cells in the APP group

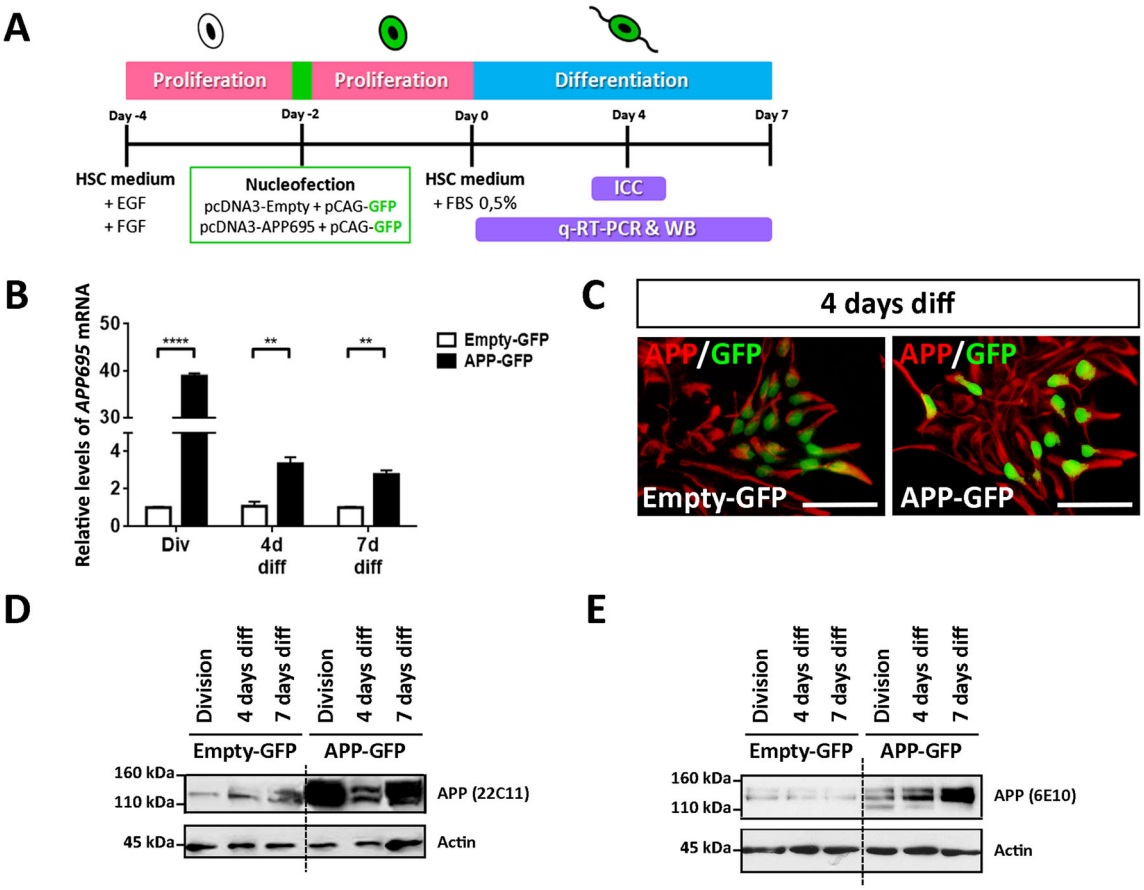

Fig. 3 APP overexpression in hNS1 cells after transient nucleofection. **a** Schematic representation of the protocol followed to overexpress APP695 in hNS1 cells. **b** Relative expression levels of *APP695* by q-RT-PCR in control hNS1 cells (Empty-GFP) and APP hNS1 cells (APP-GFP) at different days after nucleofection (division, days 4 and 7). Data represent mean ± S.E.M. ($n = 3$ for each experiment; results were confirmed in two independent experiments). Statistical analysis was performed using Student's *t* test between control and APP groups; $^{**}p < 0.01$; $^{****}p < 0.0001$. **c** APP overexpression was confirmed by APP staining in control hNS1 cells (Empty-GFP) and APP hNS1 cells (APP-GFP) after 4 days of differentiation. Scale bar = 50 μm. **d**, **e** Western blot analysis of APP695 (using 22C11 (**d**) and 6E10 (**e**) antibodies) in cellular extracts of control hNS1 cells (Empty-GFP) and APP hNS1 cells (APP-GFP) at different days after nucleofection (division, days 4 and 7). Actin was used as a loading control

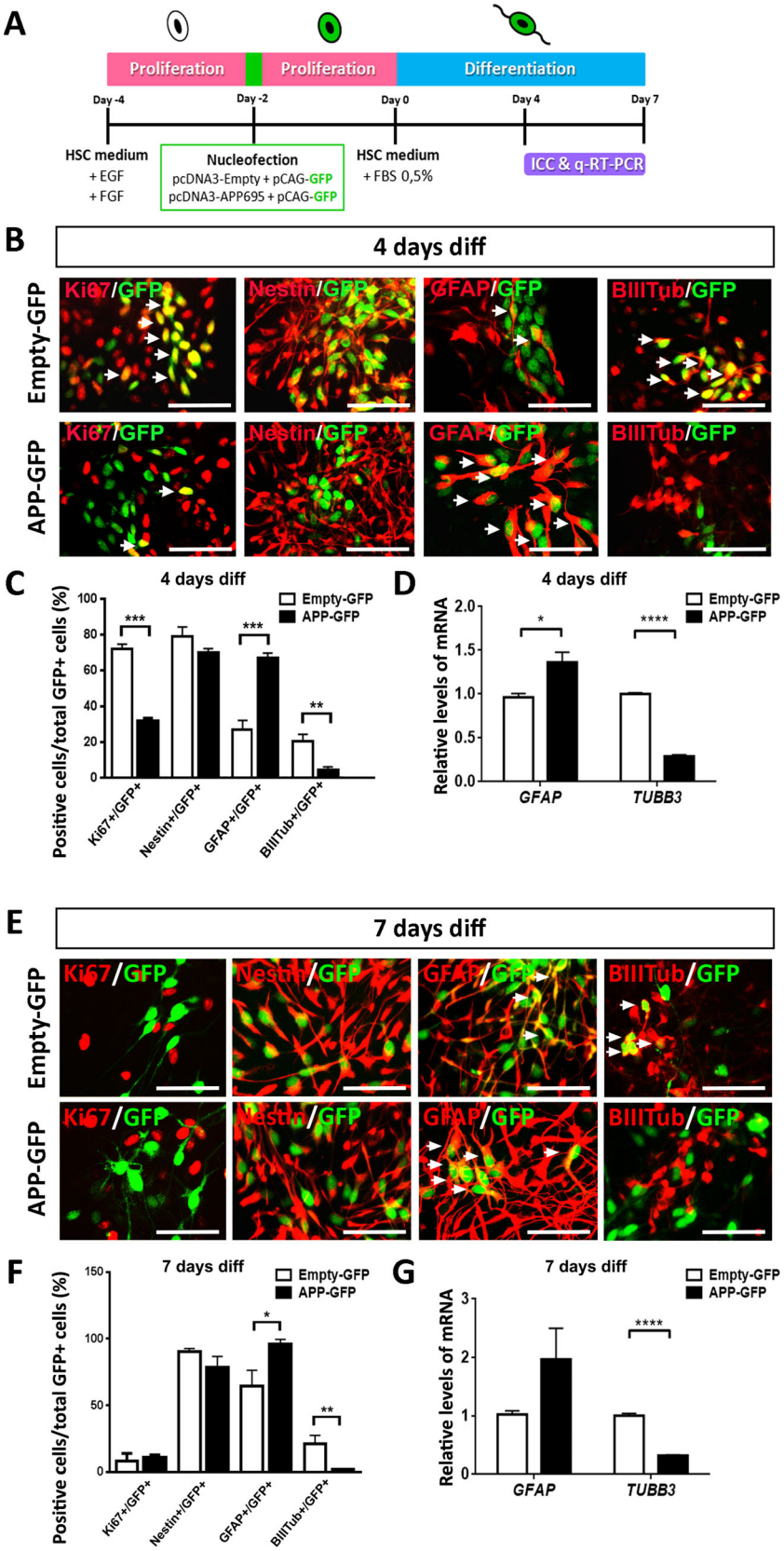

were GFAP$^+$/GFP$^+$ as compared to 65.3 ± 7.4% in the control group ($p < 0.05$; $n = 4$) and 1.6 ± 0.3% of cells were BIIITub$^+$/GFP$^+$ of APP cells as compared to 21.3 ± 3.1% of control cells ($p < 0.01$; $n = 4$). No statistical differences were observed for

◀ **Fig. 4** Effects of APP overexpression on cell fate decisions of hNS1 cells. **a** Schematic representation of the protocol. **b**, **e** Representative images at day 4 (**b**) and day 7 (**e**) of differentiation, showing immunoreactivity for Ki-67, Nestin, GFAP, and B-III-Tubulin in control hNS1 cells (Empty-GFP) and APP hNS1 cells (APP-GFP). Arrows indicate examples of co-localization between the different markers and GFP. Scale bar = 50 μm. **c**, **f** Percentage of GFP^+ cells stained for the different markers relative to the total GFP^+ cells corresponding to both experimental groups (Empty-GFP and APP-GFP) at day 4 (**c**) and day 7 (**f**) of differentiation. Data represent mean ± S.E.M. ($n = 4$ for each experiment; results were confirmed in two independent experiments). Statistical analysis was performed using Student's *t* test between control and APP groups; $*p < 0.05$; $**p < 0.01$; $***p < 0.001$. **d**, **g** Relative expression levels of *GFAP* and *TUBB3* by q-RT-PCR in control hNS1 cells (Empty-GFP) and APP hNS1 cells (APP-GFP) at day 4 (**d**) and day 7 (**g**) of differentiation. Data represent mean ± S.E.M. ($n = 3$ for each experiment; results were confirmed in two independent experiments). Statistical significance of the Student's *t* test between control and APP groups; $****p < 0.0001$

Nestin, consistent with our results at day 4 of differentiation. In addition, there were no statistical differences for Ki67 immunostaining after 7 days of differentiation, possibly because most cells have already exited the cell cycle by this time (Fig. 4e, f). These results were confirmed at the level of mRNA expression by q-RT-PCR analyses for *GFAP* and *TUBB3* (Fig 4 g). We observed a consistent trend showing an increase in *GFAP* expression, but statistically significant differences were not observed. However, it is important to note that for the purpose to studying intrinsic effects, we are mainly interested in GFP^+ cells, which are the ones overexpressing APP. Furthermore, APP overexpression in this study is transient, and, therefore, begins to decrease as differentiation progresses. For this reason, at day 7 of differentiation, the effects analyzed for *GFAP* expression may be less prominent. This effect was also observed at day 7 of differentiation when immunostaining of $GFAP^+/GFP^+$ cells described above, where at differentiation day 7, the statistical differences between both groups (control and APP) were less pronounced than at day 4 of differentiation.

Molecular Effects of APP Overexpression in hNS1 Cells

To determine the possible role of AICD on the phenotypic specification previously observed, we characterized the presence of this fragment in the two experimental groups. For immunocytochemistry (ICC) analysis, we used a rabbit antibody raised against the C-terminal domain of APP (APP-CT) (Fig. 2a) where AICD is localized. APP-CT staining was faint in control cells but intense in APP cells, with APP-CT located mainly in cell nuclei (Fig. 5b). Co-localization of APP-CT with GFP was analyzed in both experimental groups. Statistically significant differences were observed between APP and control groups, where 54.6 ± 5.7% of cells in the APP group were $APP\text{-}CT^+/GFP^+$, and only 4.1 ± 0.8% of cells in the control group were $APP\text{-}CT^+/GFP^+$ ($p < 0.001$; $n = 3$) (Fig. 5c). These results were confirmed by WB analysis, showing greater APP-CT levels at day 4 of differentiation in the APP group as compared to the control group (Fig. 5d). This indicates a higher level of AICD in the APP group as compared to the control group, illustrating the relevance of increasing APP levels in the present paradigm.

Since AICD can translocate to the nucleus and regulate the expression of several genes, we decided to analyze the expression of some of the best known target genes of AICD, as previously described [1, 2, 19]. Cell samples were collected of proliferating cells, as well as at differentiation days 4 and 7 (Fig. 5a). RT-PCR assays were done with primers specifically designed to detect *ADAM10* (ADAM metallopeptidase domain 10; the most important enzyme with α-secretase activity), *BACE1* (β-site APP cleaving enzyme 1; also known as β-secretase 1), *GSK3B* (glycogen synthase kinase 3β; isoform to GSK-3), and the endogenous gene *GAPDH* (glyceraldehyde-3-phosphate dehydrogenase) for semi-quantitative analysis. No differences were observed in the gene expression for *ADAM10* and *BACE1* between APP and control groups (data not shown). However, APP overexpressing cells showed a significant increase in the expression of *GSK3B* mRNA as compared to controls ($p < 0.05$; $n = 3$) (Supplementary Fig. 3). The results obtained for *ADAM10*, *BACE1*, and *GSK3B* were further confirmed by q-RT-PCR in proliferating and differentiating cells (days 4 and 7). We also examined the expression of *GSK3A* (glycogen synthase kinase 3α) by q-RT-PCR (Fig 5e). Unlike the expression obtained for *GSK3B*, *GSK3A* mRNA levels were unaltered and do not appear to be regulated by APP overexpression.

This increase in expression of *GSK3B* mRNA in APP overexpressing cells was confirmed at the protein level by WB analysis using an antibody against GSK-3β (Fig. 5f).

To evaluate the involvement of GSK-3β in the observed effects of APP overexpression on the phenotypic specification in hNS1 cells, control and APP groups were treated during differentiation (from 0 to 4 days) with CHIR99021, an aminopyrimidine derivative that is a potent inhibitor of GSK-3. Two different concentrations were used, 3 and 5 μM (Fig 6a).

Phenotypic analysis of GFP^+ cells in the control group revealed that 12.8 ± 5.5 and 11.7 ± 6.9% were $BIIITub^+$ in untreated and DMSO conditions, respectively. This percentage increased in the CHIR99021-treated cells to 38.7 ± 3.2% at 3 μM and 41.0 ± 2.1% at 5 μM ($p < 0.0001$; $n = 3$). However, a reverse effect was observed in the percentage of $GFAP^+/GFP^+$ cells. 32.1 ± 2.2 and 29.2 ± 2.6% of cells GFP^+ were $GFAP^+$ in untreated and DMSO groups, respectively, and 9.1 ± 3.9% (CHIR 3 μM) and 10.2 ± 3.6% (CHIR 5 μM) of cells were $GFAP^+$ in treated cells ($p < 0.0001$; $n = 3$) (Fig. 6b, c).

Similar effects, but enhanced, were obtained in the phenotypic analysis of GFP^+ cells in the APP group. 5.5 ± 1.5 and 7.5 ± 0.2% of GFP^+ cells were $BIIITub^+$ in the untreated and DMSO groups, respectively, while this percentage increased

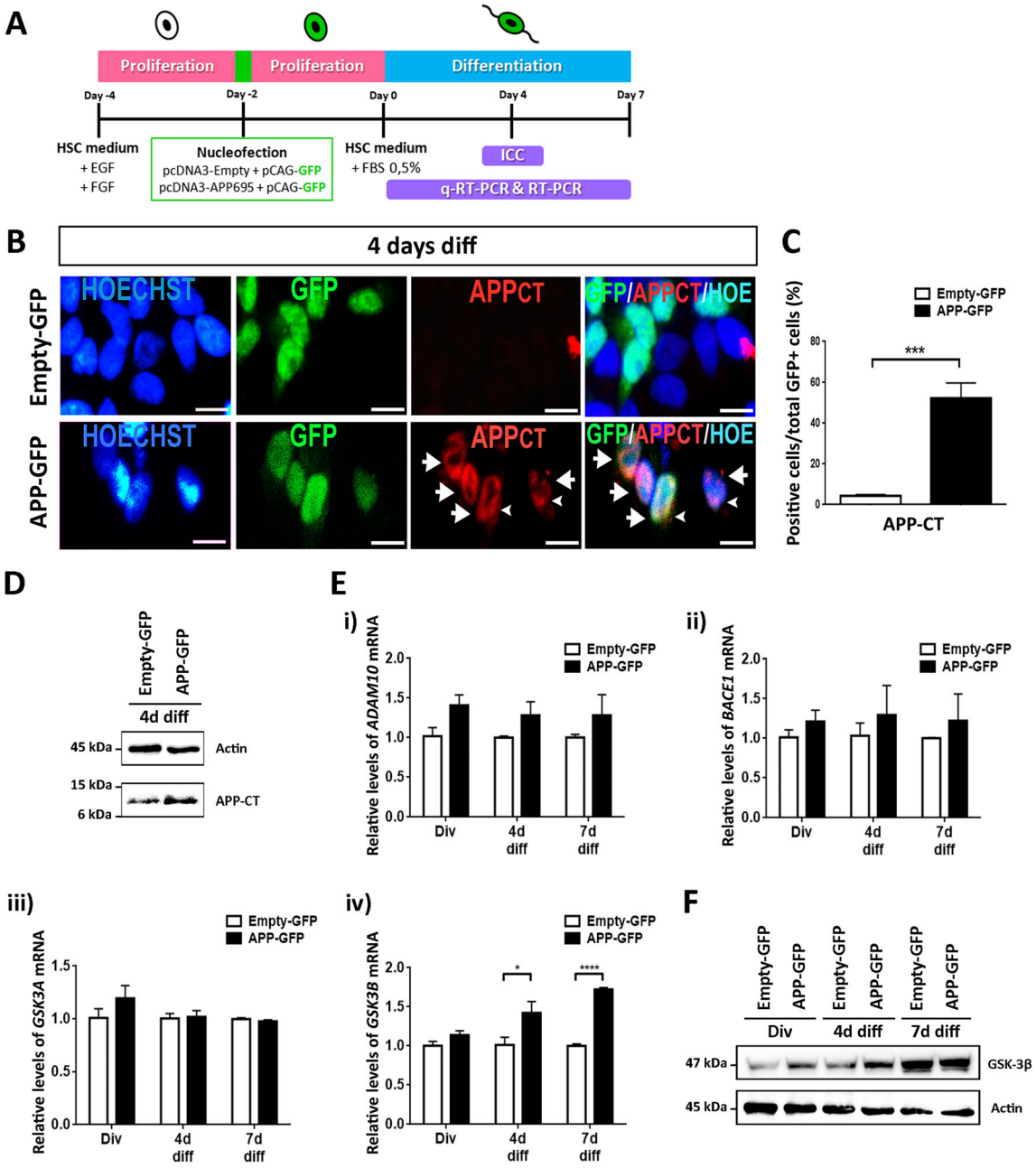

Fig. 5 Molecular effects of APP overexpression in hNS1 cells. **a** Schematic representation of the protocol. **b** Representative immunofluorescence images for detection of APP-CT in control hNS1 cells (Empty-GFP) and APP hNS1 cells (APP-GFP) after 4 days of differentiation. Arrows indicate examples of co-localization between the different markers and GFP; arrowheads indicate a slight staining for APP-CT in the cytoplasm of some cells. Scale bar = 10 μm. **c** Percentage of GFP^+ cells stained for APP-CT relative to total GFP^+ cells corresponding to both experimental groups (Empty-GFP and APP-GFP) at day 4 of differentiation. Data represent mean ± S.E.M. ($n = 3$ for each experiment; results were confirmed in two independent experiments). Statistical analysis was performed using Student's *t* test between control and APP groups; $^{***}p < 0.001$. **d** Western blot analysis of APP-CT in cellular extracts of control hNS1 cells (Empty-GFP) and APP hNS1 cells (APP-GFP) at day 4 of differentiation. Actin was used as a loading control. **e** Relative expression levels of *ADAM10* (i), *BACE1* (ii), *GSK3A* (iii), and *GSK3B* (iv) by q-RT-PCR in control hNS1 cells (Empty-GFP) and APP hNS1 cells (APP-GFP) at different days after nucleofection (division, days 4 and 7). Data represent mean ± S.E.M. ($n = 3$ for each experiment; results were confirmed in two independent experiments). Statistical analysis was performed using Student's *t* test between control and APP groups; $^{*}p < 0.05$; $^{****}p < 0.0001$. **f** Western blot analysis of GSK-3β in cellular extracts of control hNS1 cells (Empty-GFP) and APP hNS1 cells (APP-GFP) at different days after nucleofection (division, days 4 and 7). Actin was used as a loading control

in the CHIR99021 treated cells to 59.8 ± 4.8% at 3 μM and 75.3 ± 3.4% at 5 μM ($p < 0.0001$; $n = 3$). The percentage of $GFAP^+/GFP^+$ cells was 57.3 ± 1.6 and 55.9 ± 1.5% in the untreated and DMSO groups, respectively, as compared to 8.0 ± 0.1% (CHIR 3 μM) and 3.2 ± 1.8% (CHIR 5 μM) in treated cells ($p < 0.0001$; $n = 3$) (Fig. 6d, e).

These results indicate that APP overexpression enhances the expression of *GSK3B* in hNS1 cells, probably mediated by the APP proteolytic product AICD. This further indicates that GSK-3β might have an important role in the phenotypic specification of hNS1 cells.

Discussion

APP is the central protein involved in AD pathology, as it is the precursor of Aβ peptide. A good understanding of the cell biology of this protein and its physiological function could allow for the generation of therapeutically relevant compounds to manage this disorder. hNSCs, being the precursors of neurons and glia of the CNS, constitute a useful tool for a better understanding of human brain development and the molecular pathology associated with a particular neurodegenerative disease. In this study, we aimed to identify the intrinsic effects of APP on the differentiation pattern and cell fate specification of hNSCs, using hNS1 cells as a model system.

Our results demonstrate that APP is expressed in dividing and differentiating hNS1 cells. These findings are consistent with previous reports in human embryonic stem cells (hESCs) [32], human telencephalic neurospheres [33], cortical GABAergic and excitatory neurons [3], and radial glia and neural progenitors of the SVZ and hippocampus of the adult brain [8, 9, 34]. Overall, the presence of APP in hNSCs suggests a functionally relevant role in the biology and differentiation of neural stem/precursor cells.

To study the possible function of APP in hNSCs, we analyzed the effects of APP gain-of-function in our cellular model. Our results indicate that transient APP overexpression induces early cell cycle exit and directs their cell fate towards a glial phenotype, while decreasing neuronal differentiation.

Some authors have proposed that APP and its metabolites are able to regulate the phenotypic specification of hNSCs. It has been demonstrated that *APP* gene transfection promotes gliogenesis rather than neuronal differentiation in hNSCs [35], which is consistent with our results. However, as we suggested above, these effects could also be mediated, at least in part, by the APP/AICD system, since higher levels of the AICD domain were observed in APP-overexpressing cells as compared to controls.

AICD is generated upon processing of APP in both the amyloidogenic and non-amyloidogenic pathways, though its physiological relevance is controversial and still not well understood. It is believed that the fragment translocates to the nucleus, where it regulates the expression of different target genes [1, 2, 19]. Interestingly, AICD levels are increased in AD brains, in trisomic Ts65Dn mice, and in human fetuses with DS [36, 37]. In addition, a regulatory role of AICD in neuroblast cell proliferation and differentiation has been proposed [22] and AICD has been shown to inhibit neurogenesis in neural stem/precursor cells through a mechanism not fully characterized [2, 25]. Recently, AICD was shown to have an indirect role in suppressing neuronal differentiation of hNSCs via transcriptional regulation of specific miRNAs, such as miR-663, which in turn suppresses the expression of several pro-neurogenic genes [24]. Furthermore, a number of in vitro studies have implicated AICD in cell signaling and transcriptional regulation of different genes including *GSK3B*, which codes for GSK-3β, a proline-directed Ser/Thr kinase that is believed to play a key role in disorders such as AD and DS [36, 38].

Our results clearly indicate that the overexpression of APP in hNS1 cells promotes the expression of GSK-3β. Accumulating evidence has begun highlighting the importance of GSK-3β signaling for NSCs proliferation and differentiation [36]. It has been reported that GSK-3β signaling is an essential mediator of homeostatic control that regulates neural progenitors during mammalian brain development. In fact, GSK-3β deletion in mice resulted in a marked hyperproliferation of neural progenitors, leading to a marked reduction in the generation of postmitotic neurons [39]. The importance of GSK-3β signaling has also been demonstrated in cultured neural progenitor cells where inhibitors of GSK-3β protect NPCs from apoptosis [40] and facilitate neural progenitor differentiation towards a neuronal phenotype [41]. Furthermore, in vivo overexpression of GSK-3β causes alterations in adult neurogenesis, leading to a depletion of the neurogenic niches and a decrease in the number of mature neurons [42].

Although further work is needed to analyze the molecular mechanisms and pathways involved in the effects of APP on hNSCs differentiation, our data may help explain previous findings demonstrating that NSCs from DS individuals or animal models differentiate into astrocytes rather than neurons [43].

In conclusion, our data indicate a role of APP in controlling the balance between the generation of neurons and glia from hNSCs, an effect likely mediated by the APP/AICD/GSK-3β pathway (Supplementary Fig. 4). This finding may have implications in the context of the biological role of APP, as well as more broadly in DS and AD research. A better understanding of these neurodevelopmental mechanisms could help to unravel the underlying cellular processes of neurodegenerative diseases and neuro-repair, thus providing an excellent opportunity for the design of innovative pharmacological or regenerative treatment options.

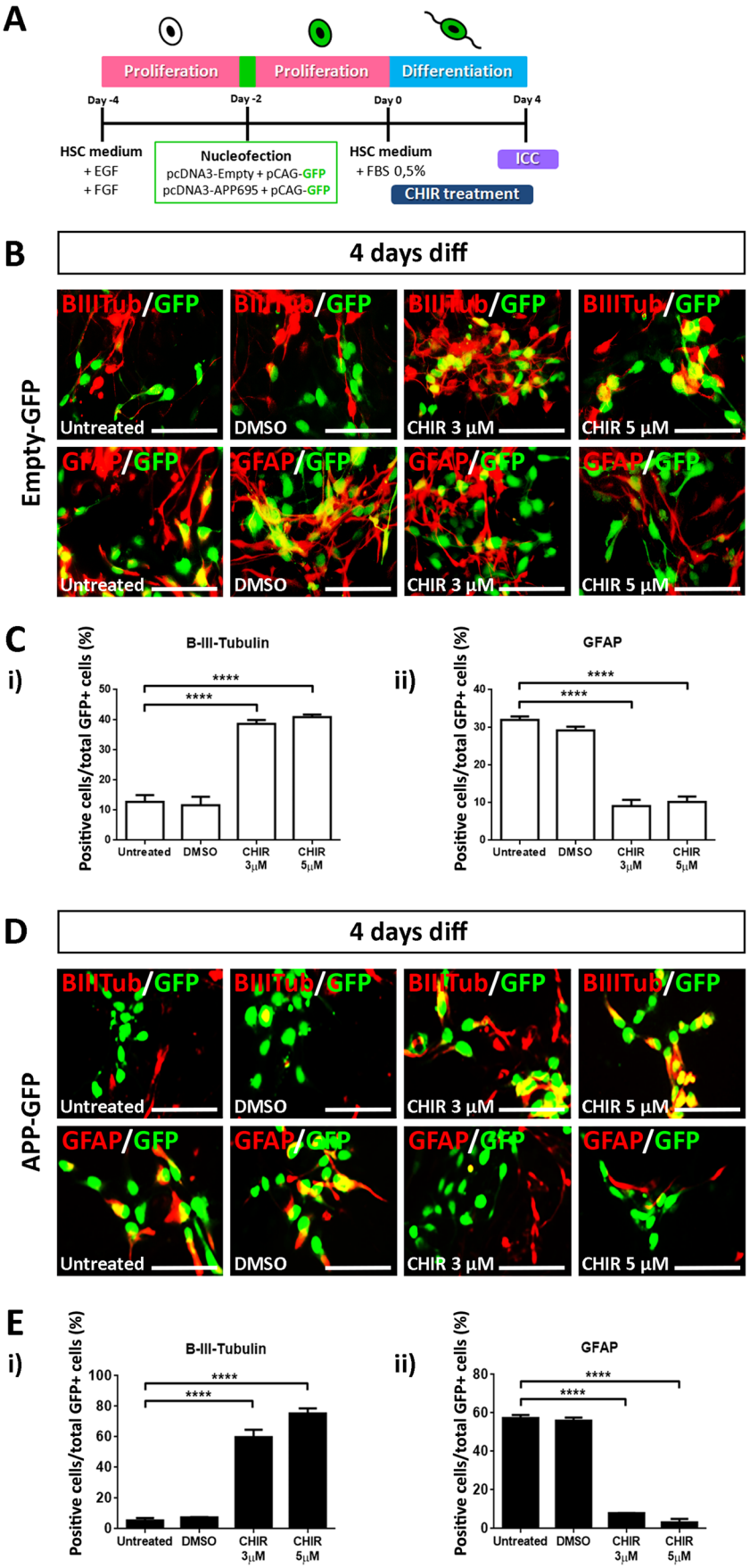
A
Proliferation
Proliferation
Differentiation
Day -4
Day -2
Day 0
Day 4
HSC medium
+ EGF
+ FGF
Nucleofection
pcDNA3-Empty + pCAG-GFP
pcDNA3-APP695 + pCAG-GFP
HSC medium
+ FBS 0,5%
ICC
CHIR treatment
B
4 days diff
Empty-GFP
BIIITub/GFP
GFAP/GFP
Untreated
DMSO
CHIR 3 µM
CHIR 5 µM
C
i)
B-III-Tubulin
ii)
GFAP
Positive cells/total GFP+ cells (%)
****
Untreated
DMSO
CHIR 3µM
CHIR 5µM
D
4 days diff
APP-GFP
E
i)
B-III-Tubulin
ii)
GFAP

◀ **Fig. 6** Effects of CHIR99021 (GSK-3 inhibitor) on cell fate decisions of hNS1 cells. **a** Schematic representation of the protocol. **b** Representative immunofluorescence images for detection of B-III-Tubulin and GFAP in control hNS1 cells (Empty-GFP) after 4 days of differentiation. Scale bar = 50 μm. **c** Percentage of GFP^+ cells stained for B-III-Tubulin (i) and GFAP (ii) relative to the total GFP^+ cells corresponding to the Empty-GFP group at day 4 of differentiation. Data represent mean ± S.E.M. ($n = 3$ for each experiment; results were confirmed in two independent experiments). Statistical analysis was performed using one-way ANOVA (multiple comparisons of each group vs untreated group); $^{****}p < 0.0001$. **d** Representative immunofluorescence images for detection of B-III-Tubulin and GFAP in APP hNS1 cells (APP-GFP) after 4 days of differentiation. Scale bar = 50 μm. **e** Percentage of GFP^+ cells stained for B-III-Tubulin (i) and GFAP (ii) relative to the total GFP^+ cells corresponding to the APP-GFP group at day 4 of differentiation. Data represent mean ± S.E.M. ($n = 3$ for each experiment; results were confirmed in two independent experiments). Statistical analysis was performed using one-way ANOVA (multiple comparisons of each group vs untreated group); $^{****}p < 0.0001$

Acknowledgements The authors wish to thank the Dr. Daniel Lu (UCLA) for providing the pcDNA.3-APP695 plasmid. We are grateful to Pilar Sáinz, Clara González, Patricia Velasco, Javier Hernández, and Cristina Gil for technical assistance.

Funding This work was supported by grants from the MICINN-ISCIII (PI-10/00291 and MPY1412/09), MINECO (SAF2015-71140-R), and Comunidad de Madrid (NEUROSTEMCM consortium; S2010/BMD-2336).

Compliance with Ethical Standards

Conflict of Interest The authors declare that they have no conflict of interest.

References

1. Dawkins E, Small DH (2014) Insights into the physiological function of the β-amyloid precursor protein: beyond Alzheimer's disease. J Neurochem 129(5):756–769
2. Zhou ZD, Chan CH, Ma QH, Xu XH, Xiao ZC, Tan EK (2011) The roles of amyloid precursor protein (APP) in neurogenesis: implications to pathogenesis and therapy of Alzheimer disease. Cell Adhes Migr 5(4):280–292
3. Müller UC, Deller T, Korte M (2017) Not just amyloid: physiological functions of the amyloid precursor protein family. Nat Rev Neurosci 18(5):281–298
4. Patterson D, Gardiner K, Kao FT, Tanzi R, Watkins P, Gusella JF (1988) Mapping of the gene encoding the beta-amyloid precursor protein and its relationship to the Down syndrome region of chromosome 21. Proc Natl Acad Sci U S A 85(21):8266–8270
5. Nalivaeva NN, Turner AJ (2013) The amyloid precursor protein: a biochemical enigma in brain development, function and disease. FEBS Lett 587(13):2046–2054
6. Van der Kant R, Goldstein LS (2015) Cellular functions of the amyloid precursor protein from development to dementia. Dev Cell 32(4):502–515
7. Kirazov E, Kirazov L, Bigl V, Schliebs R (2001) Ontogenetic changes in protein level of amyloid precursor protein (APP) in growth cones and synaptosomes from rat brain and prenatal expression pattern of APP mRNA isoforms in developing rat embryo. Int J Dev Neurosci 19(3):287–296
8. Caillé I, Allinquant B, Dupont E, Bouillot C, Langer A, Müller U, Prochiantz A (2004) Soluble form of amyloid precursor protein regulates proliferation of progenitors in the adult subventricular zone. Development 131(9):2173–2181
9. Wang B, Wang Z, Sun L, Yang L, Li H, Cole AL, Rodriguez-Rivera J, Lu HC et al (2014) The amyloid precursor protein controls adult hippocampal neurogenesis through GABAergic interneurons. J Neurosci 34(40):13314–13325
10. Tyan SH, Shih AY, Walsh JJ, Maruyama H, Sarsoza F, Ku L, Eggert S, Hof PR et al (2012) Amyloid precursor protein (APP) regulates synaptic structure and function. Mol Cel Neurosci 51(1–2):43–52
11. Wang Z, Wang B, Yang L, Guo Q, Aithmitti N, Songyang Z, Zheng H (2009) Presynaptic and postsynaptic interaction of the amyloid precursor protein promotes peripheral and central synaptogenesis. J Neurosci 29(35):10788–10801
12. Milward EA, Papadopoulos R, Fuller SJ, Moir RD, Small D, Beyreuther K, Masters CL (1992) The amyloid protein precursor of Alzheimer's disease is a mediator of the effects of nerve growth factor on neurite outgrowth. Neuron 9(1):129–137
13. Young-Pearse TL, Bai J, Chang R, Zheng JB, LoTurco JJ, Selkoe DJ (2007) A critical function for beta-amyloid precursor protein in neuronal migration revealed by in utero RNA interference. J Neurosci 27(52):14459–14469
14. Bolós M, Hu Y, Young KM, Foa L, Small DH (2014) Neurogenin 2 mediates amyloid-β precursor protein-stimulated neurogenesis. J Biol Chem 289(45):31253–31261
15. Hu Y, Hung AC, Cui H, Dawkins E, Bolós M, Foa L, Young KM, Small DH (2013) Role of cystatin C in amyloid precursor protein-induced proliferation of neural stem/progenitor cells. J Biol Chem 288(26):18853–18862
16. López-Toledano MA, Shelanski ML (2004) Neurogenic effect of beta-amyloid peptide in the development of neural stem cells. J Neurosci 24(23):5439–5444
17. López-Toledano MA, Shelanski ML (2007) Increased neurogenesis in young transgenic mice overexpressing human APP (Sw, Ind). J Alzheimers Dis 12(3):229–240
18. Jin K, Galvan V, Xie L, Mao XO, Gorostiza OF, Bredesen DE, Greenberg DA (2004) Enhanced neurogenesis in Alzheimer's disease transgenic (PDGF-APPSw, Ind) mice. Proc Natl Acad Sci U S A 101(36):13363–13367
19. Chasseigneaux S, Allinquant B (2012) Functions of Aβ, sAPPα and sAPPβ: similarities and differences. J Neurochem 120(1): 99–108
20. Freude KK, Penjwini M, Davis JL, LaFerla FM, Blurton-Jones M (2011) Soluble amyloid precursor protein induces rapid neural differentiation of human embryonic stem cells. J Biol Chem 286(27): 24264–24274
21. Porayette P, Gallego MJ, Kaltcheva MM, Bowen RL, VadakkadathMeethal S, Atwood CS (2009) Differential processing of amyloid-beta precursor protein directs human embryonic stem cell proliferation and differentiation into neuronal precursor cells. J Biol Chem 284(35):23806–23817
22. Zhou F, Gong K, Song B, Ma T, van Laar T, Gong Y, Zhang L (2012) The APP intracellular domain (AICD) inhibits Wnt signaling and promotes neurite outgrowth. Biochim Biophys Acta 1823(8):1233–1241
23. Bukhari H, Glotzbach A, Kolbe K, Leonhardt G, Loosse C, Müller T (2017) Small things matter: Implications of APP intracellular domain AICD nuclear signaling in the progression and pathogenesis of Alzheimer's disease. Prog Neurobiol 156:189–213
24. Shu R, Wong W, Ma QH, Yang ZZ, Zhu H, Liu FJ, Wang P, Ma J et al (2015) APP intracellular domain acts as a transcriptional regulator of miR-663 suppressing neuronal differentiation. Cell Death Dis 6:e1651

25. Ma QH, Futagawa T, Yang WL, Jiang XD, Zeng L, Takeda Y, Xu RX, Bagnard D et al (2008) A TAG1-APP signaling pathway through Fe65 negatively modulates neurogenesis. Nat Cell Biol 10(3):283–294
26. Martínez-Morales PL, Revilla A, Ocaña I, González C, Sainz P, McGuire D, Liste I (2013) Progress in stem cell therapy for major human neurological disorders. Stem Cell Rev 9(5):685–699
27. Lindvall O, Kokaia Z (2010) Stem cells in human neurodegenerative disorders—time for clinical translation? J Clin Invest 120(1):29–40
28. Martínez-Morales PL, Liste I (2012) Stem cells as in vitro model of Parkinson's disease. Stem Cells Int 2012:980941, 1, 7.
29. Liste I, García-García E, Martínez-Serrano A (2004) The generation of dopaminergic neurons by human neural stem cells is enhanced by Bcl-XL, both in vitro and in vivo. J Neurosci 24(48):10786–10795
30. Liste I, García-García E, Bueno C, Martínez-Serrano A (2007) Bcl-XL modulates the differentiation of immortalized human neural stem cells. Cell Death Differ 14(11):1880–1892
31. Villa A, Snyder EY, Vescovi A, Martínez-Serrano A (2000) Establishment and properties of a growth factor-dependent, perpetual neural stem cell line from the human CNS. Exp Neurol 161(1):67–84
32. Porayette P, Gallego MJ, Kaltcheva MM, Meethal SV, Atwood CS (2007) Amyloid-beta precursor protein expression and modulation in human embryonic stem cells: a novel role for human chorionic gonadotropin. Biochem Biophys Res Commun 364(3):522–527
33. Lee IS, Jung K, Kim IS, Park KI (2013) Amyloid-β oligomers regulate the properties of human neural stem cells through GSK-3β signaling. Exp Mol Med 45:e60
34. Yasuoka K, Hirata K, Kuraoka A, He JW, Kawabuchi M (2004) Expression of amyloid precursor protein-like molecule in astroglial cells of the subventricular zone and rostral migratory stream of the adult rat forebrain. J Anat 205(2):135–146
35. Kwak YD, Brannen CL, Qu T, Kim HM, Dong X, Soba P, Majumdar A, Kaplan A et al (2006) Amyloid precursor protein regulates differentiation of human neural stem cells. Stem Cells Dev 15(3):381–389
36. Trazzi S, Fuchs C, De Franceschi M, Mitrugno VM, Bartesaghi R, Ciani E (2014) APP-dependent alteration of GSK3β activity impairs neurogenesis in the Ts65Dn mouse model of Down syndrome. Neurobiol Dis 67:24–36
37. Ghosal K, Vogt DL, Liang M, Shen Y, Lamb BT, Pimplikar SW (2009) Alzheimer's disease-like pathological features in transgenic mice expressing the APP intracellular domain. Proc Natl Acad Sci U S A 106(43):18367–18372
38. Cai Z, Zhao Y, Zhao B (2012) Roles of glycogen synthase kinase 3 in Alzheimer's disease. Curr Alzheimer Res 9(7):864–879
39. Kim WY, Wang X, Wu Y, Doble BW, Patel S, Woodgett JR, Snider WD (2009) GSK-3 is a master regulator of neural progenitor homeostasis. Nat Neurosci 12(11):1390–1397
40. Jaeger A, Baake J, Weiss DG, Kriehuber R (2013) Glycogen synthase kinase-3beta regulates differentiation-induced apoptosis of human neural progenitor cells. Int J Dev Neurosci 31(1):61–68
41. Kim JS, Chang MY, Yu IT, Kim JH, Lee SH, Lee YS, Son H (2004) Lithium selectively increases neuronal differentiation of hippocampal neural progenitor cells both in vitro and in vivo. J Neurochem 89(2):324–336
42. Fuster-Matanzo A, Llorens-Martín M, Sirerol-Piquer MS, García-Verdugo JM, Avila J, Hernández F (2013) Dual effects of increased glycogen synthase kinase-3β activity on adult neurogenesis. Hum Mol Genet 22(7):1300–1315
43. Bahn S, Mimmack M, Ryan M, Caldwell MA, Jauniaux E, Starkey M, Svendsen CN, Emson P (2002) Neuronal target genes of the neuron-restrictive silencer factor in neurospheres derived from fetuses with Down's syndrome: a gene expression study. Lancet 359(9303):310–315